archives
of thermodynamics
Vol. **40**(2019), No. 1, 115–126
DOI: 10.24425/ather.2019.128293

Investigation of non-Fourier thermal waves interaction in a solid material

MARCIN LENARCZYK*
ROMAN DOMAŃSKI

Institute of Aviation al. Krakowska 110/114, 02-256 Warsaw, Poland

Abstract In this paper, effects of non-Fourier thermal wave interactions in a thin film have been investigated. The non-Fourier, hyperbolic heat conduction equation is solved, using finite difference method with an implicit scheme. Calculations have been carried out for three geometrical configurations with various film thicknesses. The boundary condition of a symmetrical temperature step-change on both sides has been used. Time history for the temperature distribution for each investigated case is presented. Processes of thermal wave propagation, temperature peak build-up and reverse wave front creation have been described. It has been shown that (i) significant temperature overshoot can appear in the film subjected to symmetric thermal load (which can be potentially dangerous for real-life application), and (ii) effect of temperature amplification decreases with increased film thickness.

Keywords: Non-Fourier equation; Heat waves; Hyperbolic heat conduction; Thermal wave interaction

Nomenclature

c_p	–	specific heat capacity at constant pressure, J/(kgK)
c_v	–	volumetric heat capacity, J/(m^{3}K)
f	–	time step number
i	–	spatial location

*Corresponding Author. Email: marcin.lenarczyk@gmail.com

L	–	film thickness, m
$\mathbf{q}(x,t)$	–	heat flux
$q(x,t)$	–	x-component of heat flux, W/m^2
$T(x,t)$	–	temperature, K
T_t	–	total duration time, s
t	–	time, s
x	–	space variable, m

Greek symbols

α	–	thermal diffusivity, m^2/s
λ	–	thermal conductivity, W/(K m)
ρ	–	density, kg/m^3
τ_q	–	relaxation time, s

Subscripts

i	–	spatial location
f	–	time level

1 Introduction

A heat wave, also known as a thermal wave, is a subject of an extensive research in thermal science and engineering. In the recent decades, one can observe a growing usage of the ultrashort-pulsed lasers (with pulse durations of the order of subpicoseconds to femtoseconds) in practical applications. At present, the thermal wave phenomenon is being applied to the fields of industrial laser heating processes, i.e., welding or non-destructive examinations, specifically the grain size and thickness of the thin metal deposits [1]. Special attention is also given to laser micromachining [2], pattering [3] as well as synthesis and processing in the thin film deposition [4]. In medicine, a heat wave propagation mechanism is being investigated [5] with some practical applications, like minimally intrusive operational techniques, which are based on heating biological tissue in a localized and safe way [6]. In chemistry, the elution chromatography is one of the examples where thermal wave phenomena is being studied [7].

Ultrashort-pulsed lasers possess exclusive capabilities in limiting the undesirable spread of the thermal process zone in the heated sample [8,9]. This advantage is widely known and it gets attention of researchers across different fields.

In the current paper, authors aim to investigate thermal effects which occur during waves interactions between each other. The numerical solution of the hyperbolic heat conduction equation is carried out for various geometrical configurations. The discussion on consequences for the material subjected to a symmetric step change of temperature is presented in the summary section.

2 Non-Fourier equation formulation

If the time of the interaction between the laser and the solid body becomes extremally small, Fourier heat conduction equation (HHC) does not provide accurate results. This is because of lack of a local thermal equilibrium [10]. In 1958 a hyperbolic heat conduction equation was proposed by Catteneo [11] and independently by Vernotte [12]. The hyperbolic equation is based on a relaxation model for heat conduction which accounts for finite thermal propagation speed. Relaxation concept addresses Fourier law's paradox of instantaneous heat propagation[1]. In the heat conduction mechanism, the thermal relaxation time plays a primary role in distinguishing the domain to be wave dominated or diffusion dominated [13].

The classical Fourier law can be written as follows:

$$q\left(x,t\right) = -\lambda \nabla T\left(x,t\right) \ , \tag{1}$$

where q is the heat flux and λ is a thermal conductivity of material. As mentioned, this equation has been modified to take into account a relaxation phenomenon

$$q\left(x,t+\tau_q\right) = -\lambda \nabla T\left(x,t\right) \ , \tag{2}$$

where τ_q is a relaxation time, which is a parameter that takes in to account the finite velocity of a thermal wave.

The classical expression for the energy equation can be written as

$$c_v \frac{\partial T(x,t)}{\partial t} = -\nabla \mathbf{q}\left(x,t\right) \ , \tag{3}$$

By introducing relaxation time in the first order approximation of the Eq. (2), we can derive formula as follows:

$$\mathbf{q}\left(x,t\right) + \tau_q \frac{\partial \mathbf{q}(x,t)}{\partial t} = -\lambda \nabla T\left(x,t\right) \tag{4}$$

[1]The paradox of instantaneous heat propagation, is not physically reasonable because it clearly violates one important principle of the Einstein's special theory of relativity: the velocity of light in vacuum is the greatest known speed and has a finite value of 2.9×108 m/s [14].

or

$$-\mathbf{q}\,(x,t) = \lambda \nabla T\,(x,t) + \tau_q \frac{\partial \mathbf{q}\,(x,t)}{\partial t}\,. \tag{5}$$

If we use this expression in the formula (3) then energy equation can be written as

$$c\frac{\partial T(x,t)}{\partial t} = \tau_q \frac{\partial}{\partial t}\left[\nabla \mathbf{q}(x,t)\right] + \nabla\left[\lambda \nabla T\,(x,t)\right]\,. \tag{6}$$

When substituting $-\nabla\mathbf{q}$ by $c(\partial T/\partial t)$ we obtain

$$c_v\left[\frac{\partial T(x,t)}{\partial t} + \tau_q \frac{\partial^2 T(x,t)}{\partial t^2}\right] = \nabla\left[\lambda \nabla T\,(x,t)\right]\,. \tag{7}$$

If additionally, we define thermal diffusivity, which is

$$\alpha = \frac{\lambda}{\rho c_p}\,, \tag{8}$$

where ρ is the density and c_p is the volumetric heat capacity, we obtain hyperbolic heat conduction equation given as

$$\frac{\partial T(x,t)}{\partial t} + \tau_q \frac{\partial^2 T(x,t)}{\partial t^2} = \alpha \frac{\partial^2 T}{\partial x^2}\,. \tag{9}$$

3 Numerical method

Let consider a very thin film with thickness considerably smaller than the length, as shown in Fig. 1. Geometrical configuration allows us to take a 1D approach. The side walls are suddenly heated with the same, constant temperature, which implies boundary conditions:

$$x = 0: \quad T(x,t)|_{x=0} = 100\,. \tag{10}$$

$$x = L: \quad T\,(x,t)|_{x=L} = 100\,. \tag{11}$$

Convection and radiation are assumed to be negligible. The film is maintained at a uniform, initial temperature $T = 0$, thus initial conditions for $t = 0$ can be written as

$$T(x,t)|_{t=0} = 0\,. \tag{12}$$

$$\left.\frac{\partial T(x,t)}{\partial t}\right|_{t=0} = 0\,. \tag{13}$$

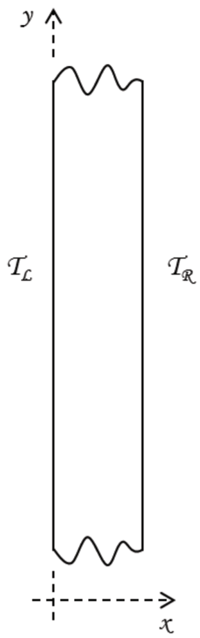

Figure 1: Considered domain with coordinate system: τ_L/τ_R – left/ride side wall temperature.

A finite difference method with an implicit scheme has been employed to solve this problem numerically. Let define a time discretization as

$$0 = t^0 < t^1 < \ldots < t^{f-1} < t^f < \ldots < t^F = T_t \tag{14}$$

and $\triangle t = t^f - t^{f-1}$, thus $t^f = f\triangle t$, where f is a time step number and $F = T_t/\Delta t$. Furthermore, 1D space domain of $x \in [0, L]$, where L is total length of the domain and N is number of nodes, can be defined as

$$0 = x_0 < x_1 < \ldots < x_{i-1} < x_i < \ldots < x_N = L \tag{15}$$

and $\triangle x_i = x_{i+1} - x_i$, assuming constant distance between spatial nodes we can consider $\triangle x = L/N$, and then $x_i = x_0 + i\triangle x$ $(i = 1, \ldots, N)$. Finite differences for derivatives of hyperbolic heat conduction Eq. (9) can be written as follows. First order time finite difference

$$\left.\frac{\partial T(x,t)}{\partial t}\right|_{x_i}^{t^f \to t^{f+1}} \cong \frac{T\left(x_i, t^{f+1}\right) - T\left(x_i, t^f\right)}{\triangle t}. \tag{16}$$

Second order finite difference of time can be written as follows:

$$\left.\frac{\partial^2 T(x,t)}{\partial t^2}\right|_{x_i}^{t^f \to t^{f+1}} \cong \frac{T\left(x_i, t^{f+1}\right)}{(\triangle t)^2} - \frac{2T\left(x_i, t^{f}\right)}{(\triangle t)^2} + \frac{T\left(x_i, t^{f-1}\right)}{(\triangle t)^2}\,. \tag{17}$$

For the implicit scheme, adapted in this study, second order spatial variable finite difference can be defined as

$$\left.\frac{\partial^2 T(x,t)}{\partial x^2}\right|_{x_i}^{t^f \to t^{f+1}} \cong \frac{T\left(x_{i+1}, t^{f+1}\right)}{(\triangle x)^2} - \frac{2T\left(x_i, t^{f+1}\right)}{(\triangle x)^2} + \frac{T\left(x_{i-1}, t^{f+1}\right)}{(\triangle x)^2}\,. \tag{18}$$

If we denote $T_i^f = T(x_i, t^f)$, then the finite difference approximation of Eq. (9) can be written in the form

$$\frac{T_i^{f+1} - T_i^f}{\triangle t} + \tau_q \frac{T_i^{f+1} - 2T_i^f + T_i^{f-1}}{(\triangle t)^2} = \alpha \frac{T_{i-1}^{f+1} - 2T_i^{f+1} + T_{i+1}^{f+1}}{(\triangle x)^2}\,. \tag{19}$$

Above equation is applicable to the inner nodes of the computational domain, $i = 1, \ldots, N-1$. For the boundary nodes temperature value is being derived directly from boundary conditions:

$$T_0^{f+1} = 100\,, \qquad f = 1, \ldots, F-1\,, \tag{20}$$

$$T_n^{f+1} = 100\,, \qquad f = 1, \ldots, F-1\,. \tag{21}$$

Equations (19), (20), and (21) create a system of algebraic equations, which can be denoted by means of matrix $\mathbf{A}$ and vectors $\mathbf{B}$ and T^{f+1}

$$\mathbf{A}T^{f+1} = \mathbf{B}\,, \tag{22}$$

which is then solved by the Gauss elimination method.

Throughout numerical calculations, the number of elements of the grid is selected to be between 1000 and 3000 to obtain a grid independent solution.

Material properties of the film are assumed to be as follows: density $\rho = 8000$ kg/m^3, specific heat capacity $c_p = 500$ J/kgK, and thermal conductivity $\lambda = 40$ W/K m [15].

4 Results

Numerical calculations have been carried out for three geometrical configurations with various film thicknesses: 10 , 20, and 30 $\times$ 10^{-9} m. All the three cases have been subjected to the identical boundary conditions, a symmetrical temperature change on both sides (described in the previous section). For each case, the same relaxation time is considered, $\tau_q = 10^{-11}$ s. Duration time has been set arbitrary for each geometrical calculation to investigate maximum temperature in the vicinity of film walls. Time history for the temperature distribution variations for each investigated case is shown in Fig. 2.

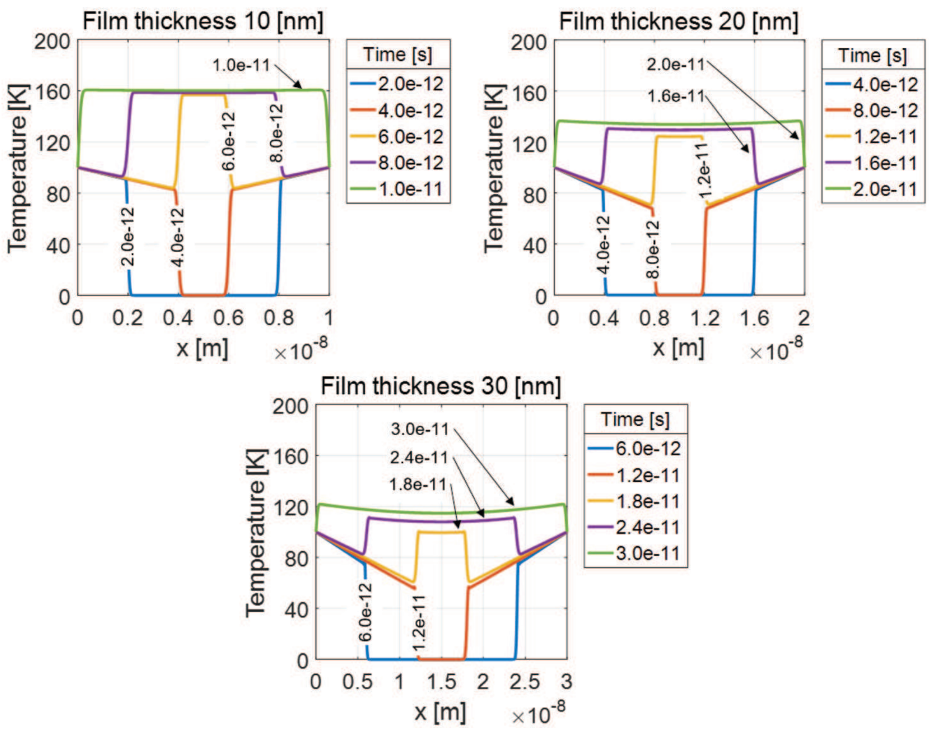

Figure 2: Temperature distribution variation. Investigated cases: 10, 20, and 30 $\times 10^{-9}$ m film thickness.

After the boundary conditions on both sides are imposed, a set of wave fronts is being created in the domain. Thermal wave propagation starts to advance toward centre. The propagation front separates the thermally affected zone from the thermally undistributed region. Once wave fronts arrive at the centre of the film they collide with each other causing sudden and significant temperature increase in this region. After that, revers thermal wave fronts emerge and they begin to advance toward side walls. Once reverse waves reach boundary region – for all the investigated cases –

the temperature at both heated walls exceed the imposed wall temperature creating temperature overshoot.

Performed numerical study predicts the existence of thermal waves providing both the amplification and shape. Large reverse waves are seen in case of thinner films. For the case of 10×10^{-9} m thickness, maximum temperature registered at the control surface – placed 1×10^{-9} m from the side wall – is equal to 161 K (see Fig. 2). Compared to 100 K imposed as a boundary condition, temperature overshoot in the vicinity of side walls is equal to 61 K. For the thicker, 20×10^{-9} m film, temperature at the control surface raised up to 136 K, while for the 30×10^{-9} m case maximum temperature was only 121 K. Figure 3 presents values of maximum temperature amplifications next to the side walls in function of time. The plot shows effect of temperature overshoot decrease with film thickness increase.

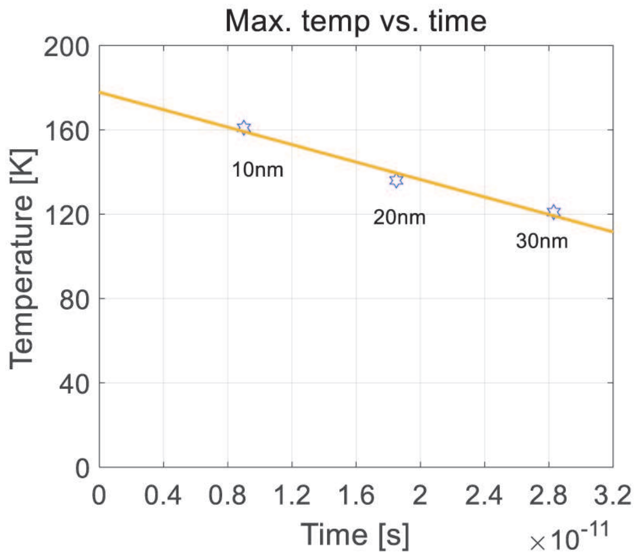

Figure 3: Maximum temperature peak value at control surface. Investigated cases: 10, 20, and 30×10^{-9} m film thickness.

In the central part of the film the temperature increases rapidly and then decreases steadily. Next to the side walls temperature overshoots appear as temporary peaks. An example can be seen in Fig. 4, which presents time history of heat propagation process for 10×10^{-9} m film. Reverse heat waves create temperature overshoots next to the side walls periodically. Each temperature peak is obviously lower than its predecessor as the en-

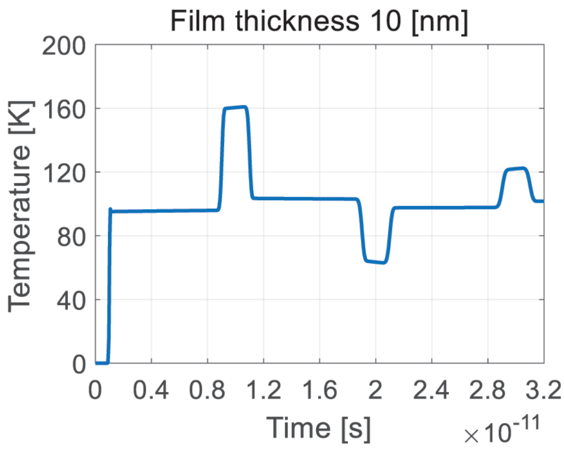

Figure 4: Time history of heat propagation process. Control point located next to the side wall. Case: 10×10^{-9} m film.

tire system moves toward equilibrium state. In Fig. 5 we can see sudden temperature changes across the 10 nm film, with temperature oscillations over temperature equilibrium value of 100 K.

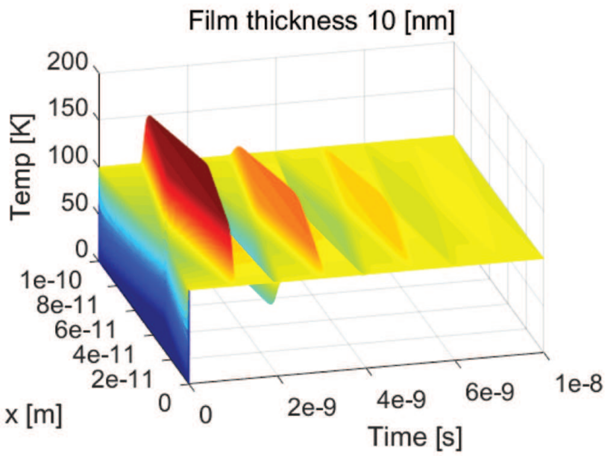

Figure 5: Temperature distribution history across film thickness. Case: 10×10^{-9} m film.

In Fig. 6 we can see a detailed evolution of the thermal waves for the 10 nm film thickness case. If we neglect wave front itself and consider only non-wave part of temperature distribution along film thickness, we can observe temperature oscillation over 100 K as well. During that process energy is being transferred to the system and from the system, due to the positive or negative sign of the thermal gradient next to the side walls.

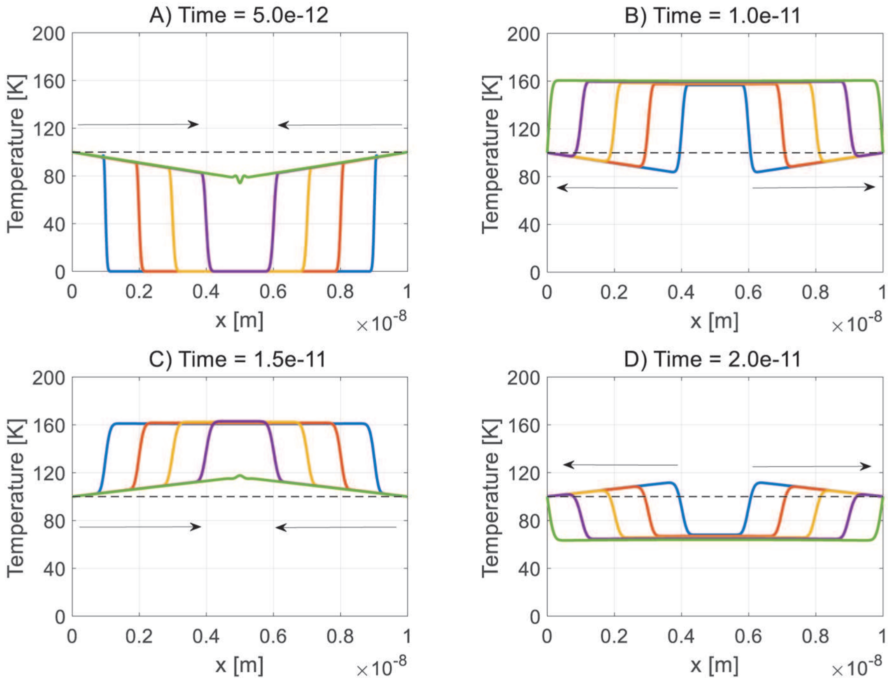

Figure 6: Thermal waves evolution over time. Arrows show waves propagation directions. Case: 10×10^{-9} m film.

5 Summary

A numerical study on heat waves interaction has been performed. The non-Fourier, hyperbolic heat conduction equation is solved using a finite difference method with an implicit scheme. Special consideration has been given to heat transfer behaviour before and after symmetrical collision of wave fronts coming from two sides of a film. It has been shown that significant temperature overshoot can appear in the film subjected to symmetric thermal load at two side walls. Effect of temperature amplification decrease with increased film thickness – for a given thermal relaxation time – has been revealed.

Results of the presented study suggest that temperature overshoot phenomena in a very thin film can be potentially dangerous for real-life applications, where strict temperature limits are imposed. However, temperature amplification effect can be significantly reduced by increasing distance between side walls and forcing wave fronts to decrease (or disappear) when they arrive at the centre of the film and then side walls.

Received 25 October, 2017

References

[1] Opsal J.: *The application of thermal wave technology to thickness and grain size of aluminum films.* In: Proc. SPIE **1596**(1991), 120–131.

[2] Knapp J.A., Borgesen P., Zuhr R.A. (Eds.): *Beam-Solid Interactions: Physical Phenomena.* Mater. Res. Soc. Symp. Proc. **157**(1990).

[3] Elliot D.J., Piwczyk B.P.: *Single and multiple pulse ablation of polymeric and high density materials with excimer laser radiation at 193 nm and 248 nm.* Mater. Res. Soc. Symp. Proc. **129**(1989), 627–636.

[4] Narayan J., Gosbole V.P., White G.W.: *Laser method for synthesis and processing of continuous diamond films onnondiamond substrates.* Science **52**(1991), 5004, 416–418.

[5] Tung M.M., Trujillo M., López Molina J.A., Rivera M.J., Berjano E.J.: *Modeling the heating of biological tissue based on the hyperbolic heat transfer equation.* Math. Comput. Model. **50**(2009), 5-6, 665–672.

[6] Manns F., Borja D., Parel J.M., Smiddy W., Culbertson W.: *Semianalytical thermal model for sub-ablative laser heating of homogeneous nonperfused biological tissue: Application to laser thermokeratoplasty.* J. Biomed. Opt. **8**(2003), 2, 288–297.

[7] Sharma K.R.: *Hyperbolic Wave Propagative Partial Differential Equation Solution in Elution Chromatography.* Abstr. Pap. Am. Chem. Soc. (2001), 79, 1.

[8] Tzou D.Y., Chen J.K., Beraun J.E.: *Hot-electron blast induced by ultrashort-pulsed lasers in layered media.* Int. J. Heat Mass Tran. **45**(2002), 16, 3369–3382.

[9] Othman M.I., Abouelregal A.E.E.: *The effect of pulsed laser radiation on a thermoviscoelastic semi-infinite solid under two-temperature theory.* Arch. Thermodyn. **38**(2017), 3, 77–99.

[10] Baumeister K.J., Hamill T.D.: *Hyperbolic heat conduction equation – A solution for the semi-infinite body problem.* J. Heat Trans. **91**(1969), 4, 543–548.

[11] Cattaneo C.: *Sulla conduzione de calore.* Atti Semin. Mat. Fis. Univ. Modena 3 **42**(1948), 83–101.

[12] Vernotte P.: *La véritable équation de la chaleur.* C.R. Acad. Sci. (Paris) **247**(1958), 2103–2105.

[13] Domański R.: *Research of the thermal conductivity of solid bodies for impulse action of the heat flux*. PhD thesis, Warsaw University of Technology, Warszawa 1976 (in Polish).

[14] Marín E.: *Does Fourier's law of heat conduction contradict the theory of relativity?*. Lat. Am. J. Phys. Educ. **5**(2011), 2, 402–405.

[15] Jaworski M.: *Energy transport into the solid medium by giantic laser pulses.* PhD thesis, Warsaw University of Thechnology, Warszawa 1998 (in Polish).